ELSEVIER

Colloids and Surfaces
A: Physicochemical and Engineering Aspects 107 (1996) 205–221

COLLOIDS AND SURFACES A

The reversibility of virus attachment to mineral surfaces

J.P. Loveland [a], J.N. Ryan [a,*], G.L. Amy [a], R.W. Harvey [b]

[a] *Department of Civil, Environmental, and Architectural Engineering, University of Colorado, Campus Box 428, Boulder, CO 80309, USA*

[b] *United States Geological Survey, Water Resources Division, 3215 Marine Street E-119, Boulder, CO 80303-1066, USA*

Received 13 March 1995; accepted 19 July 1995

Abstract

Virus transport through groundwater is limited by attachment to mineral surfaces and inactivation. Current virus transport models do not consider the implications of the reversibility of virus attachment to minerals. To explore the reversibility of virus attachment to mineral surfaces, we attached PRDI, a bacteriophage considered to be a good model of enteric viruses, to quartz and ferric oxyhydroxide-coated quartz surfaces over a range of pH values in equilibrium "static columns." Following attachment, we detached the viruses by replacing the pore solution with solutions of equal and higher pH. The extent of virus attachment followed an attachment "edge" that occurred at a pH value about 2.5-3.5 pH units above the pH_{IEP} of the mineral surfaces. Viruses attached below this edge were irreversibly attached until the pH of the detachment solution exceeded the pH value of the attachment edge. Viruses attached above this edge were reversibly attached. Derjaguin-Landau-Verwey-Overbeek (DLVO) potential energy calculations showed that the attachment edge occurred at the pH at which the potential energy of the primary minimum was near zero, implying that the position of the primary minimum (attractive or repulsive) controlled the equilibrium distribution of the viruses. The results suggest that the reversibility of virus attachment must be considered in virus transport models for accurate predictions of virus travel time.

Keywords: Colloids; Colloid transport; Ferric oxyhydroxide coating; PRD1; Quartz surfaces; Virus attachment; Virus release; Virus transport

1. Introduction

Half of the population of the United States relies on groundwater for drinking water supply [I]; however, only about half of these public water supply systems are reducing microbial pathogen occurrence by disinfection and treatment [2]. Owing to the proximity of some of these groundwater supplies to anthropogenic sources of microbial pathogens, including leaking septic tanks and sewage lines, groundwater recharge with waste water effluent, and land application of sludge [3,4], and the lack of adequate disinfection, untreated groundwater was responsible for one-third of the waterborne outbreaks of disease in recent decades [5]. Viruses are believed to be the most disinfection-resistant microbial pathogen and exhibit the most conservative transport behavior [2]. Virus transport in groundwater is limited by (1) virus removal through inactivation, or the loss of infective capability; (2) virus removal by irreversible attachment to mineral surfaces; and (3) virus retardation by reversible attachment to mineral surfaces.

Virus attachment to aquifer sediments is primar-

* Corresponding author.

SSDI 0927-7757(95)03373-4

ily controlled by electrostatic interactions between surfaces [3,4,6-10]. Viruses are colloid-sized particles composed of capsid proteins encapsulating infectious genetic material (nucleic acids). Surface charge on viruses is caused by ionization of the typical amino acid groups that comprise proteins. Surface functional groups on these amino acids are dominated by carboxyl and amine groups, which yield viruses with amphoteric surfaces and pH_{IEP} values (the pH at which the net surface charge is zero) ranging from 3 to 7 [11]; thus, viruses may be positively or negatively charged in natural waters. Because most aquifer grain surfaces are negatively charged in the pH range of natural waters (pH 4-9), virus transport at pH values below the pH_{IEP} of the virus will be limited by attachment. At pH values above the virus pH_{IEP}, both virus and mineral surfaces are negatively charged and removal by attachment will be diminished. However, certain minerals (e.g. sesquioxides, carbonates) are positively charged in the pH range of natural waters. These minerals, although low in abundance, have high surface areas and will significantly affect virus transport [10-16].

Virus transport through groundwater can be modeled in the same way that colloid filtration theory represents the interactions of Brownian colloids with "collector" surfaces [17,18]. The attachment of colloids to surfaces depends on the hydrodynamics of colloid approach to the surface (quantified by the single collector efficiency, n) and the surface chemical interactions between approaching colloid and surface (quantified by the collision efficiency, a). The interactions between surfaces are characterized by the Derjaguin-Landau-Verwey-Overbeek (DLVO) potential energy [19,20]. The DLVO profile between like-charged surfaces is typically characterized by (1) the primary maximum, the energy barrier to attachment and detachment; (2) the primary minimum, the deep energy "well" located close to the surface; and (3) the secondary minimum, the shallow energy well located some distance away from the surface (Fig. 1a). A vastly different DLVO profile results in the case of oppositely charged surfaces or at high ionic strengths; only the primary minimum exists and the profile is attractive at all separation distances (Fig. 1b).

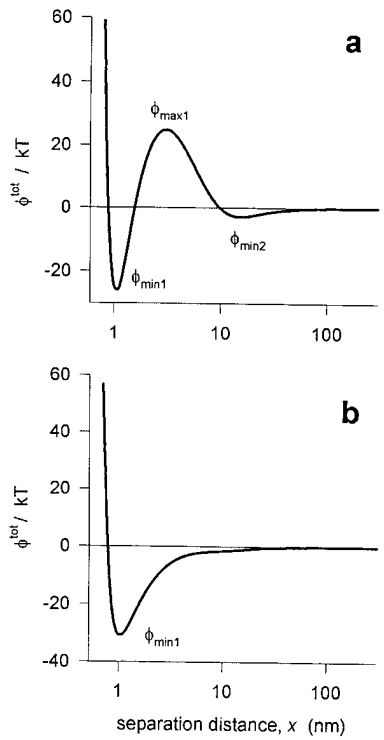

Fig. 1. Plots of the intersurface potential energy between two surfaces as a function of separation distance. (a) This potential energy profile is typical of the case where significant electrostatic repulsion exists between the surfaces. The primary minimum, Φ_{min1}, is very close to the surface, while the secondary minimum, Φ_{min2}, is much further away. Separating the two is a repulsive energy barrier, the primary maximum, Φ_{max1}. (b) This potential energy profile is typical of the case where either electrostatic attraction reinforces van der Waals attraction between the surfaces (between oppositely charged surfaces) or where van der Waals attraction exceeds a repulsive electrostatic component yielding a sum total interaction that is still attractive (between like-charged surfaces). There is no barrier to attachment and no secondary minimum, Φ_{min2}.

Colloid attachment in the primary minimum is typically considered to be irreversible without substantial perturbation of solution chemistry resulting in highly repulsive conditions [21,22]. Similar behavior has been observed for virus attachment, with changes in pH or surface modifications required to promote release [23,24]. The magnitude of the energy barrier to detachment ($-(\phi_{max1}-\phi_{min1})$) typically is much greater than the average thermal energy possessed by the colloids; therefore, the kinetics of detachment are

expected to be extremely slow [25]. In contrast, colloid attachment in the secondary minimum has been hypothesized to be reversible because the depth of the secondary minimum (ϕ_{min2}) is comparable to the thermal energy possessed by the colloids [26,27].

The reversibility of virus attachment is an important factor in predicting virus transport. Completely irreversible attachment leads to eventual attenuation of the virus plume, while viruses undergoing completely reversible attachment are retarded but not attenuated. Depending on the composition of the mineral surface, reversible and irreversible attachment has been observed for poliovirus to several oxide and metal surfaces in equilibrium batch experiments [13]. In column transport studies, Bales et al. [23,24] observed reversible virus attachment; however, virus detachment was much slower than virus attachment, suggesting that neither completely irreversible nor completely reversible attachment describes virus transport. Harvey and Garabedian [28] found that bacterial transport through an aquifer was best described by a combination of irreversible and reversible attachment terms that represent bacterial deposition in the primary and secondary minimum, respectively.

The goal of this research was to explore the reversibility of virus attachment as a function of solution pH and mineralogy of the porous media. We hypothesized that viruses attached in the absence of an energy barrier inhibiting attachment would be irreversibly attached because they would be attached in a deep primary minimum (Fig. 2). Subsequently, a substantial increase in solution pH would be required to increase electrostatic repulsion and detach the viruses. Viruses attached in the presence of an energy barrier would predominantly be reversibly attached in the secondary minimum and their detachment would exhibit a greatly reduced dependence on solution pH. To test these hypotheses, we attached the bacteriophage PRD1 to quartz and ferric oxyhydroxide-coated quartz surfaces at pH values ranging from 3 to 9. Following attachment, we detached the viruses in solutions of equal or higher pH ranging up to pH 11. The attachment and detachment results were compared to DLVO potential energy profiles calculated for the PRDI-mineral systems over the range of pH values tested.

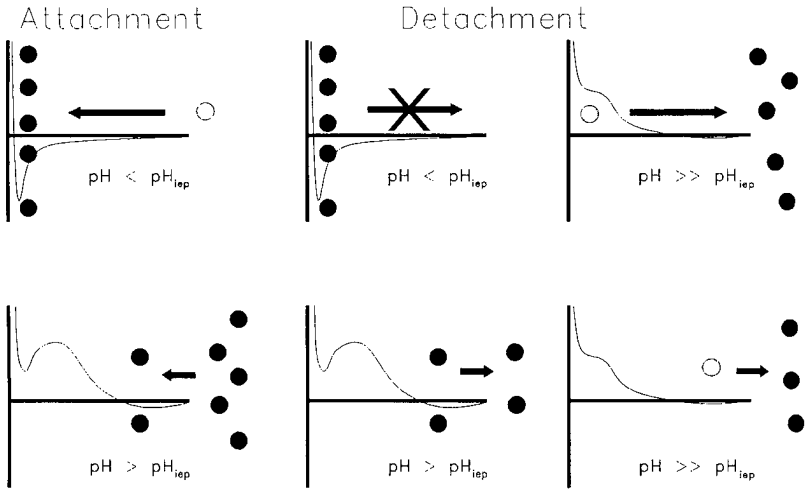

Fig. 2. Hypothesized mechanisms of virus attachment and detachment related to chemical conditions and hypothetical DLVO profiles. (a) Attachment is nearly complete where a net attractive potential energy profile exists, and detachment cannot occur until the near-surface region is sufficiently repulsive. (b) Attachment under repulsive conditions where a barrier to attachment exists. Attachment is minimal and occurs in the secondary minimum and detachment is possible because of the shallow depth of the secondary minimum.

2. Methods

2.1. Materials

Viruses

The bacteriophage **PRD1** was used as a model for naturally occurring pathogenic enteric viruses. Bacteriophages are similar to enteric viruses in size, shape, and surface characteristics [29]. PRDI, originally isolated from Kalamazoo, Michigan sewage [30], has a diameter of 62 nm and a hydrophobic lipid layer beneath its protein capsid [31]. PRDI has a reported pH_{IEP} of slightly less than 4 determined by microelectrophoresis in a buffer containing 10^{-4} M calcium and phosphate [23].

Significant variability (± 30% of the mean of replicate plates) in the standard plaque assay for this phage [32] and the concomitant difficulty in determining the extent of virus attachment led us to develop methods to radiolabel the PRD1 for enumeration using liquid scintillation. Radiolabeling also affords the benefit of allowing for the determination of total virus concentrations rather than infective virus concentrations, the result of the plaque assay technique. Murray and Parks [13] note that this is a very important distinction when attempting to model the attachment and detachment of viruses within a thermodynamic framework because the surface coverage of attached viruses can be determined. The ratio of total to infective virus particles has been found to be on the order of 10^2-10^4 [13].

PRD1 was cultured by infecting *Salmonella typhimurium* grown in a dextrose or glucose growth media deficient in methionine (DMEM; ICN Biomedicals) at a multiplicity of infection (MOI) of 5. The PRD1 virions were radiolabeled by adding 50 mCi/L of a ^{35}S-labeled methioninecysteine compound (Tran^{35}S-Label^{TM}, ICN Biomedicals) 5 min after infection [31,33]. The culture was incubated until the host cells ruptured (lysis) and released new viruses (approximately 2 h). The culture was then centrifuged in a Sorvall RC-5B with a GSA rotor for 15 min at 10 000 rev /min to remove cellular debris. Any remaining debris was removed by filtering through 0.2 μm cellulose acetate bottle filters (Corning). The PRD1 was then pelleted by centrifuging for 6 h at 20 000 rev /min in a Sorvall SS-23 rotor and resuspended by sequentially washing each tube with 5 ml of phosphate-buffered saline (PBS; ionic strength I=0.140M; 0.9 mM KH_2P0_4; 6.4 mM $NaHPO_4$).

Rate-zonal centrifugation was performed to assure that the radiolabeled and infectious viruses were isolated in the same fractions E33]. The resulting suspension was layered on top of a 5-20% (w/v) sucrose step gradient formed by hand and centrifuged for 45 min at 23 000 rev min^{-1} and 23ºC in the SW41 rotor of a Beckman ultracentrifuge [31]. The centrifuge tubes were fractionated into I ml samples, and assayed for titer and radioactivity. The peak fractions were coincident (Fig. 3) and were pooled and dialyzed (Spectra/Por 1 dialysis tubing) overnight three times against a four-hundredfold volume of PBS.

The radioactive count rates (counts per minute, or cpm) were measured by a Beckman LS3801 liquid scintillation counter following the manufacturer's instructions for ^{31} S. Aliquots of 2 ml were added to 5 ml of Ultima Gold XR scintillation cocktail (Packard) and counted for 15 min. This cocktail has a very high aqueous loading capacity (about 50%) and yielded excellent counting effi-

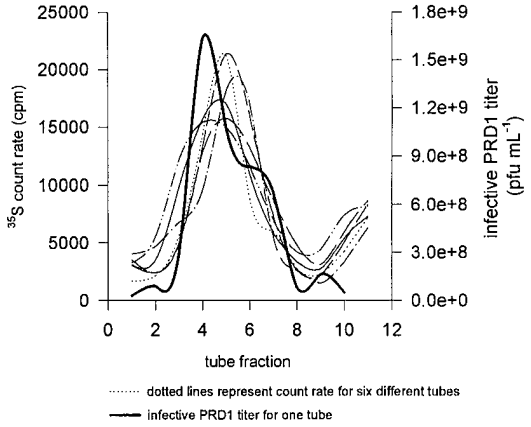

Fig. 3. Results of the rate-zonal separation of PRDI. Fractions were collected from the bottom of the centrifuge tube (1, bottom; 11, top). Coincidence of the ^{35}S radioactivity peak with the infectivity peak demonstrates that a majority of the full, intact PRD1 virions were radiolabeled. The secondary peak at the top of the tube probably represents unincorporated radiolabel and protein fragments. Fractions 4, 5 and 6 were pooled for dialysis and used in the experiments.

ciencies (≥97%) and small uncertainties (≤5%). Background counts that arose from the high incidence of solar radiation at increased elevation were measured by counting an equivalent volume of electrolyte solution and subtracting from the total count rate.

The total virus particle concentration was determined by converting the absorbance at 260 nm of the stock suspension to the total PRD1 concentration using a conversion factor based on the extinction coefficient of the proteins in poliovirus and the molecular weight of PRD1 [34-36]. The total PRD1 concentration was then correlated to the radioactivity to allow the measurement of PRD1 concentrations via liquid scintillation counting of experimental suspensions. Total PRD1 concentrations were used to determine the equilibrium surface coverage based on a geometric space-filling model of the equivalent spherical surface area of the mineral and the projected spherical area of the virus.

Minerals

Quartz grains (99% pure as determined by the supplier, Aldrich Chemical) of size fraction 210-297 μm were used as one of the porous media. The surfaces of the quartz grains were prepared by washing 300 g in 800 ml of 0. 1 M NaOH for 3 h on a shaker bench [37] and rinsing 3 times with Milli-Q water (Millipore, 18.2 MS2 resistivity). The procedure was then repeated with 0.1 M $HN0_3$. The order of the base and acid wash was switched if the pH of the experiment was greater than 7.

Quartz grains coated with ferric oxyhydroxides (referred to as Fe-quartz) were formed by adding anhydrous FeCl3 to a quartz suspension and precipitating iron oxyhydroxides at high pH with the addition of NaOH [38,39]. The sand was then dried at 105ºC overnight, rinsed through a 297 μm sieve to remove colloidal and fine particulate iron, and dried again at 105ºC. Fe-quartz particles for powder X-ray diffraction analysis were concentrated by filtering a suspension of fine particles isolated from the coated grains through a 0.45 μm membrane filter. The suspension was created by sedimentation of the coated grains in MilliQ water.

Electrophoretic mobilities for the quartz and Fe-quartz were determined by laser Doppler-shift velocimetry (Brookhaven Zeta-Plus zeta potential analyzer) and converted to zeta potentials using the Smoluchowski equation. Nine mobility measurements in the experimental solutions at 25ºC were used to report a mean and standard deviation for each pH. The quartz suspension used for analysis was produced by crushing some quartz grains with a mortar and pestle and resuspending them in the experimental solution. The Fe-quartz suspension created for the X-ray diffraction analysis was diluted for the electrophoretic mobility measurements.

Static columns

Attachment and detachment experiments were conducted in 20 ml glass syringes (Popper & Sons) according to procedures adapted from bacterial attachment experiments [37] (Fig. 3). These "static columns" were soaked for 3 h in a 0.1 M NaOH bath to dissolve any residual radioactive viruses, rinsed with Milli-Q water, and then soaked for 3 h in a 0.1 M HCl bath to remove trace metals. Residual organic matter was finally oxidized by baking the columns for 6 h at 450ºC in a Thermodyne 62700 furnace. The same acid and base cleaning procedures were used for the 105 mm polypropylene mesh (Spectramesh) used to hold the grains in the columns and the PVC stopcocks (Cole-Parmer) used to drain off the interstitial sample.

The use of static columns has several advantages in mechanistic studies of colloid attachment and detachment behavior. Static columns allow the equilibrium determination of the fraction of viruses attached for a solid-solution ratio similar to that found in a natural system versus the very low solid-solution ratio typical of stirred batch experiments. The absence of an energy input from stirring ensures that Brownian diffusion is the only mechanism transporting PRD1 to the mineral surface. However, static column experiments are limited by the absence of a hydrodynamic flow field and the lack of a tangential component of the groundwater flow velocity, which may alter the equilibrium distribution of the viruses near the mineral surfaces.

2.2. Experimental procedure

Experiments were designed to measure the equilibrium distribution of PRD1 between the mineral surface and the bulk solution as a function of the attachment and release pH. All experiments were conducted using the same solid-solution ratio and initial virus concentration. To evaluate the behavior of PRD1 over a wide range of surface interactions, the solution pH was varied with HNO_3 or NaOH from pH 3 through 11 for the quartz experiments and from pH 4 to 9 for the Fe–quartz experiments. Fluctuations in pH were maintained with various inorganic and biological buffers (Sigma Chemical): sodium acetate (pK_a 4.7), HEPES (*n*-(2-hydroxyethyl) piperazine-*N*′-(2-ethanesulfonic acid), pK_a 7.5), and CHES (2-(*N*-cyclohexylamino)-ethanesulfonic acid, pK_a 9.3). An ionic strength between 1×10^{-3} M and 2×10^{-3} M was maintained with 10^{-3} M $NaNO_3$ and 10^{-3} M of the appropriate buffer. This range of solution chemistry covers pH values both above and below the expected pH_{IEP} of PRD1 and the Fe–quartz. The pH of individual samples were measured (3 ml sample, Orion Ross® combination electrode and Orion 720A meter) after sampling to account for slight changes in pH caused by mineral dissolution.

Attachment experiments were conducted by rapidly adding a known mass of mineral grains into virus suspensions of known PRD1 concentration contained in a series of static columns buffered at the same pH (Fig. 4). These viruses were allowed to equilibrate overnight. Previous kinetic virus attachment experiments demonstrated that attachment was rapid, with a majority of the viruses attaching in less than I h, and equilibrium was reached within 5 It [33]. A series of virus-free solutions ranging in pH from the attachment pH to pH 11 and increasing in increments of 1 pH unit was then added to the series of columns. To obtain a sample of the equilibrated virus suspension, a volume slightly less than the interstitial pore volume was then drawn off and counted to establish the amount of viruses left in solution. The difference in concentration was assumed to be attached on the surface and was determined according to

$$\frac{V_0 - V_{fl}}{V_0} \times 100 = \text{PRD1} \quad \text{attached (\%)}$$

where V_0 is the initial virus concentration and V_{fl} is the sampled virus concentration. The remaining interstitial volume and a small volume of the added virus-free solution was then withdrawn and discarded, leaving only the virus-free solution in contact with the mineral grains. The columns were again allowed to equilibrate overnight and the interstitial concentration was then sampled to establish the amount of viruses detached at the various pH values. All attachment and detachment experiments were conducted at 10°C by placing

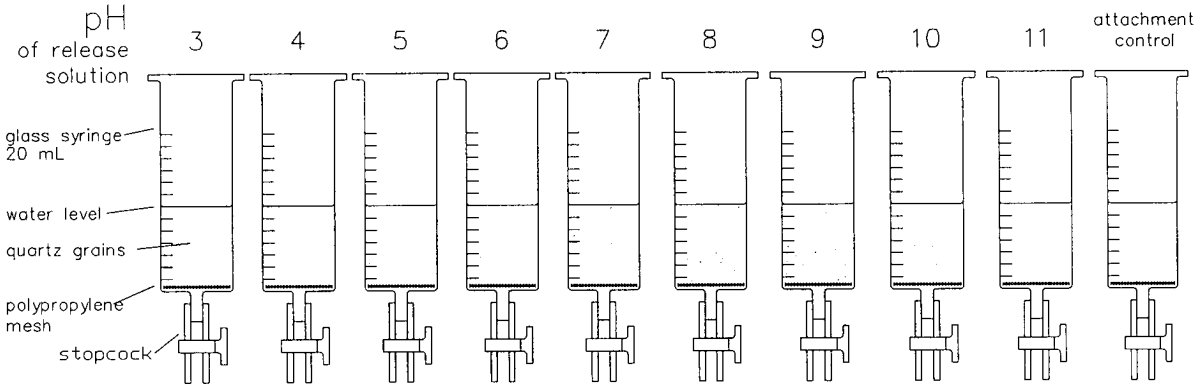

Fig. 4. Schematic of experimental apparatus showing multiple reaction static columns and experimental procedure. This particular set of static columns represents a set of experiments where the PRD1 was attached at pH 3 in all of the columns and detached in increasing increments of I pH unit in successive columns.

the static columns in an incubator prior to and during the experiments.

In the higher pH attachment and detachment solutions, the initial pH value was not always maintained by the buffers. In the presence of quartz, the pH decreased by about I unit when the initial pH value was 9.0 or above. In the presence of Fe-quartz, the pH decreased by as much 2 units at the highest initial pH of 11.0. The size of the decrease increased with the initial pH value. We suspect that the pH decrease was caused by consumption of OH -by quartz dissolution and proton release from surface Fe-OH groups.

2.3. Experimental controls

Two types of controls were performed: (1) an attachment control; and (2) an elution control. The attachment control consisted of a column, maintained for the duration of the attachment experiment, containing the virus suspension without mineral grains added. This control measured the amount of PRD1 attached to the columns walls and the polypropylene mesh. None of the attachment controls exhibited virus removals of ≥ 5%. Given the small variability in the scintillation measurement, most virus removals were zero.

The elution control consisted of adding a virus free solution to the column after the various samples were withdrawn and immediately sampling this volume to test if any viruses were eluted by passing the solution through the matrix. No virus elution took place; all elution control sample concentrations were zero within the error of the scintillation measurement.

2.4. DLVO potential energy calculations

To assess the nature of virus interactions with mineral surfaces, we calculated DLVO potential energy profiles for the experimental conditions used. To quantify these interactions, we expressed the intersurface potential energy as the sum of van der Waals, double layer, and Born potential energies over the separation distance x (m) between the approaching surfaces

$$\Phi^{\mathrm{tot}}(x)=\Phi^{\mathrm{vdW}}(x)+\Phi^{\mathrm{dl}}(x)+\Phi^{\mathrm{Born}}(\mathrm{x})$$

The double layer potential energy (Φ^{dl} (J)) was calculated using the following expression [40] adapted from that of Hogg et al. (HHF; [41]) for sphere–plate geometry

$$\Phi^{\mathrm{dl}}(x)=\pi\epsilon\epsilon_0 r_c\left[2\psi_c\psi_g \ln\left(\frac{1+e^{-\kappa x}}{1-e^{-\kappa x}}\right)+(\psi_c^2+\psi_g^2)\ln(1-e^{-2\kappa x})\right] \quad (3)$$

where ϵ is the dielectric constant of water, (dimensionless), ϵ_0 is the permittivity of free space, (C V^{-1} M^{-1}), r_c is the radius of the colloid (virus) (m), ψ_c is the surface potential of the colloid (virus) (V), ψ_g is the surface potential of the mineral grain (V), and κ is the inverse Debye–Hückel length (m^{-1}), which is given by

$$\kappa=\left[\frac{2IN_A1000e^2}{\epsilon\epsilon_0k_BT}\right]^{-1/2} \quad (4)$$

in which N_A is Avogadro's number, e is the elementary charge (C), k_B is the Boltzmann constant (J K^{-1}), and T is the temperature (K). Owing to linearization of the Poisson–Boltzmann equation, the HHF expression is limited to surface potentials less than 60 mV [25]. Given the relatively low ionic strength of these experiments, we assumed that the measured zeta potentials were reasonable surrogates for surface potentials.

The van der Waals potential energy (Φ^{vdW} (J)) for retarded sphere–plate interactions was calculated using the expression derived by Gregory [42] as

$$\Phi^{\mathrm{vdW}}(x)=-\frac{A_{123}r_c}{6x}\left[1+\left(\frac{14x}{\lambda}\right)\right]^{-1} \quad (5)$$

where A_{123} is the complex Hamaker constant (J) and λ is the "characteristic wavelength" of the interaction, usually taken as 10^{-7} m. Murray and Parks [13] approximated the complex Hamaker constant for poliovirus interactions with mineral surfaces from the self-interaction Hamaker constants obtained from Lifshitz theory using an equation derived by Bargeman and van Voorst Vader [43]. These values of A_{123} for the poliovirus–quartz–water system (0.4×10^{-20} J) and the poliovirus–hematite–water system (0.75×10^{-20} J) were

used as the values of A_{123} for the PRD1–mineral–water systems.

Two approaches were used to account for repulsion arising from electron orbital overlap and to provide a primary minimum of finite depth: (1) the Born potential energy; and (2) a minimum separation distance. The Born potential energy (Φ^{Born} (J)), the repulsive component of the same interatomic potentials that give rise to the van der Waals potential energy [44], was formulated as [25]

$$\Phi^{Born}(x)=\frac{A_{123}\sigma^6}{7560}\left[\frac{8r_c+x}{(2r_c+x)^7}+\frac{6r_c-x}{x^7}\right] \quad (6)$$

where σ (Å) is the Born collision parameter. The commonly used value of $\sigma=5$Å [25,45] was adopted for these experiments. The Born potential, a "soft" interatomic potential expression, is the least well understood interaction potential. The Born collision parameter has been used as a fitting parameter to explain experimental data of colloidal detachment phenomena [22]. A minimum separation distance, the analog of the interatomic "hard-sphere" potential [44], of 10 Å was selected to approximate the separation distance of the overlap of the shear plane at which the zeta potential is assumed to be measured. The distance to the shear plane has been estimated at about 5 Å, the thickness of the first few layers of water immobilized on charged surfaces [46,47]. Minimum separation distances of 4–10 Å have been determined from the results of colloid release experiments [48–51]. Using $\sigma=5$Å in the Born potential energy expression (Eq. 6) results in an effective minimum separation distance of about 2–3 Å.

3. Results

3.1. Zeta potential measurement

Microelectrophoresis revealed that the particle suspension isolated from the quartz grains was negatively charged over the range of experimental pH values (Fig. 5). This result fits the expected pH_{IEP} of a quartz suspension of about 2.5 [52].

The particle suspension isolated from the Fe–quartz grains had a pH_{IEP} of approximately 5.1

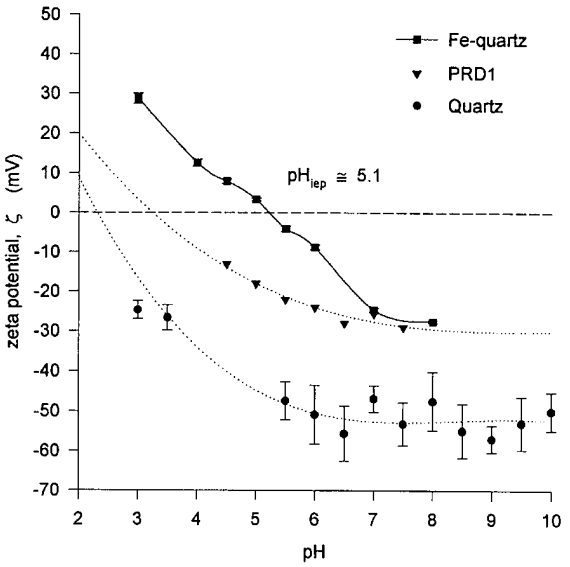

Fig. 5. Plots of zeta potential (ζ) of quartz, Fe–quartz, and PRD1 as a function of pH. The cubic polynomial curve fits for quartz and PRD1 predict pH_{IEP} values of 2.5 and 3.5, respectively. The PRD1 data are taken from Bales et al. [23].

(Fig. 5). The Fe-quartz particle suspension showed a large X-ray diffraction peak for quartz and smaller peaks for akagan6ite (β–FeOOH) and other forms of hydrous ferric oxides. The measured pH_{IEP} falls roughly half-way between the pH_{IEP} values expected for quartz (about 2.5) and ferric oxyhydroxides (7-8) [52]. The abundance of quartz in this suspension suggests that the measured pH,,, is lower than that of pure ferric oxyhydroxides because the suspension is a mixture of the quartz and ferric oxyhydroxides; however, we are not certain that this suspension is representative of the grain surfaces. The measured pH_{IEP} may also be caused by the incorporation of silica in the ferric oxyhydroxide, which precipitated at high pH in the presence of quartz.

Zeta potentials for the PRD1 for use in DLVO calculations were obtained from Bales et al. [23], who measured the pH_{IEP} of PRD1 in a solution containing 10^{-4} M calcium and phosphate. Our experiments were conducted in the presence of indifferent electrolytes; therefore, our experimental pH_{IEP} for PRD1 may be somewhat different.

3.2. Calculated DLVO profiles

The calculated intersurface potential energy between quartz and PRD1 is attractive at all separation distances at pH 3 (Fig. 6a). At pH 7 and 9, the DLVO profile is repulsive at all separation distances. At pH 9, the primary minimum vanishes if the minimum separation distance is considered. The intersurface potential energy between PRD1 and the Fe-quartz is attractive at all separation distances at pH 4.4 (Fig. 6b). At pH 5.9-6.6, the DLVO profiles exhibit barriers to attachment and attractive primary minima. At pH 7.3 and above, the DLVO profiles exhibit repulsive potential energy at all separation distances. For these DLVO profiles, secondary minima were present but extremely small. The secondary minima depths were on the order of 10^{-3} k_BT.

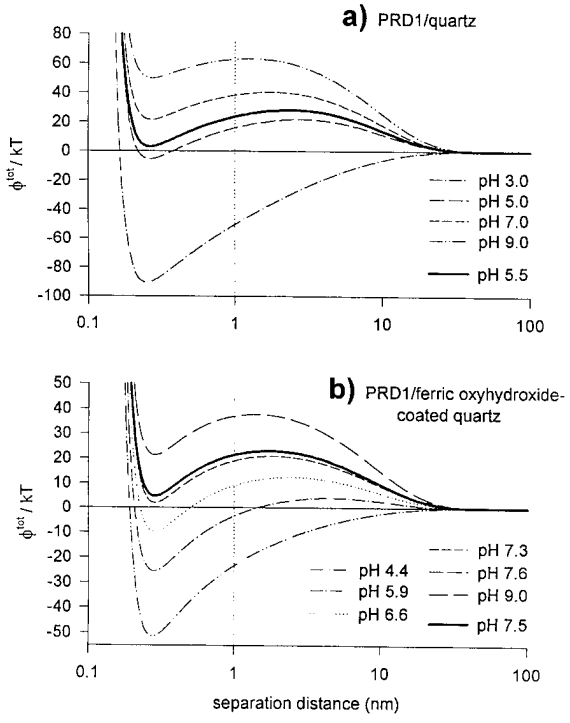

Fig. 6. Plots of the DLVO potential energy profiles for PRDI-mineral surface interactions. The dotted vertical line at a I nm separation distance represents a minimum separation distance. (a) DLVO potential energy for PRD1-quartz. (b) DLVO potential energy for PRD1-Fe-quartz.

3.3. PRD1 attachment to quartz

PRD1 was attached to quartz surfaces at pH values of approximately 3.0, 5.0, 7.0, and 9.0 (Fig. 7a). PRD1 attachment at pH 3.0 and 5.0 was nearly complete (greater than 90%), while attachment at pH 7.0 and 9.0 was minimal (below 10%). Given the small error of the scintillation measurements, attachment at pH 3.0 and 5.0 was significantly different from 100% within a confidence interval of 2σ.

Using the estimates of total PRD1 obtained by relating the light absorbance to the ^{35}S count rate, fractional surface coverage by attached PRD1

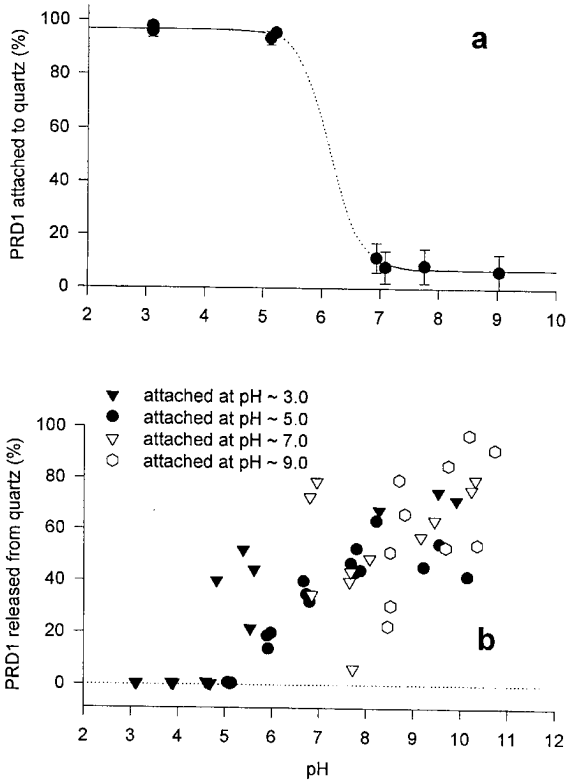

Fig. 7. PRD1 attachment to and detachment from quartz grains as a function of pH. (a) Attachment edge for PRD1 to quartz grains. (b) Detachment of PRDI. from quartz grains. Filled symbols represent irreversibly attached viruses; i.e. viruses that remained attached when the pH of the detachment solution was the same as the pH of the attachment solution. Empty symbols represent reversibly attached viruses, i.e. viruses that detached when the pH of the detachment solution was the same as the pH of the attachment solution.

never exceeded 10^{-7} [33]. For similar initial virus concentrations of the smaller (27 nm diameter) and less negatively charged poliovirus, Murray and Parks [13] observed fractional surface coverages of about 10' on quartz. For these calculations, we assumed that single PRD1 virions were attaching to the mineral surfaces and that virus aggregation was not occurring even at the lowest pH values. For the initial virus concentrations used in these experiments (10^5–10^6 pfu ml $^{-1}$), Grant [5 3] predicted that virus aggregation is much slower than virus inactivation. For PRDI. at 10ºC, the temperature of these experiments, virus inactivation is a slow process (a log-order reduction in virus titer occurs on the order of at least days [54]); therefore, PRD1 aggregation is not expected.

3.4. PRD1 detachiment from quartz

PRD1 was detached from the quartz surface at final pH values ranging from the pH of attachment to pH 11 (Fig. 7b). For PRD I attached at pH 3, detachment initiated at pH 4.9. For PRD1 attached at pH 5, detachment initiated at about pH 5.5. Above these pH values, the amount of PRD1 detached increased with the pH of the detachment solution. PRD I attached to quartz at pH 7 and 9 were detached to the solution at the same pH values at which they were attached. Again, the amount of PRD1 detached increased with increasing pH.

At high pH values, relatively small amounts of PRD1 were attached to the quartz surfaces. When we measured the detachment of this small amount of PRDI, the ^{35}S count rate was not far above background; therefore, we attribute the large scatter in the amount of PRDI detached at the higher pH values to the relatively small amount of PRDI attached at these pH values.

3.5. PRDI attachment of ferric oxyhydroxidecoated quartz

PRD1 was attached to the Fe-quartz grains at pH values ranging from 4.4 to 9.0 (Fig. 8a). Attachment was nearly complete below pH 7.0. At pH 9, attachment did not occur. Surface coverage by PRD1 on the Fe-quartz grains was of similar magnitude (about 10^{-7}) to that observed on the pure quartz, assuming that the ferric oxyhydroxide coating did not substantially increase the grain radius used to calculate the geometric surface area available for attachment.

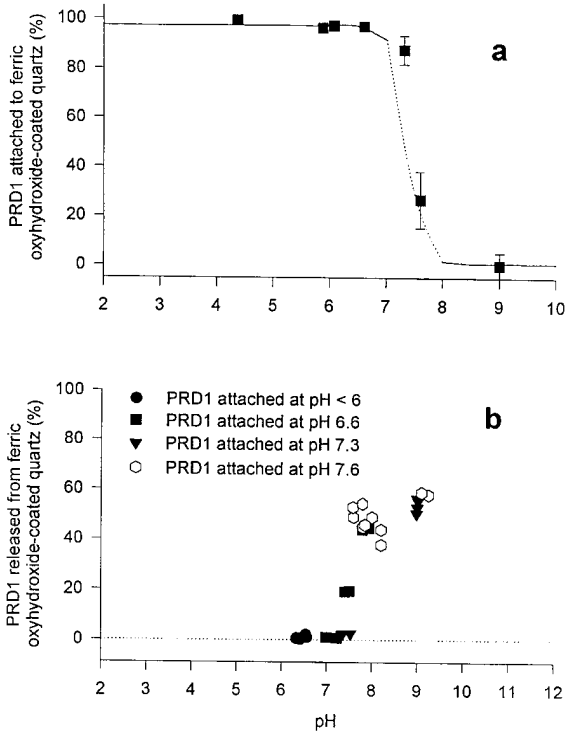

Fig. 8. PRDI attachment to and detachment from Fe-quartz grains as a function of pH. (a) Attachment edge for PRDI to Fe-quartz. (b) Detachment of PRDI from the Fe-quartz grains. Filled symbols represent irreversibly attached viruses; i.e. viruses that remained attached when the pH of the detachment solution was the same as the pH of the attachment solution. Empty symbols represent reversibly attached viruses, i.e. viruses that detached when the pH of the detachment solution was the same as the pH of the attachment solution.

3.6. PRD1 detachment from ferric oxyhydroxidecoated quartz

PRDI was detached from the surface at final pH values ranging from pH 6 to 9.5 (Fig. 8b). For PRD1 attached below pH 7.3, detachment did not occur until the pH of the detachment solution exceeded pH 7.5. For PRDI attached at pH 7.6, detachment occurred at the pH of attachment.

PRD1 detachment from the Fe-quartz grains increased with increasing pH of the detachment solution in a manner similar to that observed in the PRD1-quartz system.

4. Discussion

4.1. PRD1 attachment behavior

The extent of PRD1 attachment to the mineral grains closely resembles typical pH sorption "edges" for anions. The **PRD1** attachment edge for quartz, defined by 50% attachment, occurs at pH 6 (± 1), about 3.5 pH units above the expected pH_{IEP} of the quartz surface (Fig. 7a). The PRD1 attachment edge for Fe-quartz occurs at pH 7.5 (± 0. 1), about 2.4 pH units about the measured pH_{IEP} of the Fe-quartz surface (Fig. 8a).

At the lowest pH values, the near-complete attachment of PRD1 is expected because the virus and mineral surfaces are oppositely charged. For PRD1-quartz at pH 3, we expect that the PRD1 is slightly positively charged and the quartz is slightly negatively charged. For PRD1-Fe-quartz at pH 4.4, the PRD1 is slightly negatively charged and the Fe-quartz is slightly positively charged.

At slightly higher pH values, but still below the attachment edge, attachment of PRD1 to the mineral surfaces occurred despite the presence of repulsive double layer forces. For example, at pH 5, both the PRD1 and the quartz are negatively charged. In terms of DLVO theory, the attractive van der Waals forces must overcome the repulsive double layer forces for attachment to occur at these pH values. At pH values above the attachment edge, both PRD1 and the mineral surfaces possess greater negative charge and attachment is minimal owing to double layer repulsive forces in excess of van der Waals forces.

The DLVO profiles calculated with the Born potential energy (Fig. 6) display repulsive primary maxima and primary minima located at attractive potential energy levels at pH 5 for PRD1-quartz and at pH 5.9-6.6 for PRD1-Fe-quartz. These profiles indicate that, at equilibrium, most of the viruses should be attached in the primary minimum. The nearly complete attachment (greater than 90%) of viruses at pH values below the attachment edges and the irreversibility of this attachment suggest that the viruses were attached in the primary minimum.

The DLVO profiles cut off at a minimum separation distance of 1 nm (refer to the dotted vertical line in Fig. 6) displayed primary minima at repulsive potential energies under the same conditions. These DLVO profiles do not adequately describe the attachment results because the equilibrium distribution resulting from the repulsive primary minima would predict little attachment in the primary minima.

4.2. Reversible PRD1 attachment

At pH values above the attachment edge, virus attachment was minimal (less than 10%). At these high pH values, the DLVO profiles calculated using the Born repulsion term displayed primary minima located at repulsive potential energies. The repulsive primary minima indicate that the majority of the viruses will not be attached in the primary minima at equilibrium. The minimal amount of virus attachment observed at high pH values agrees with this result. Attachment in the presence of repulsive barriers has typically been attributed to secondary minimum deposition. Coagulation theory and experiments showing the dependence of the stability ratio on colloid size have provided evidence in support of the existence of the secondary minimum and its role in coagulation [26,27]. Following this evidence, deposition in the secondary minimum has been proposed as an explanation of reversible bacterial attachment [28]. On the other hand, Elimelech and O'Melia [40] argued that colloids purportedly trapped in the secondary minimum would be carried to the stagnation point at the rear of the collector grain, where adequate space exists for only a few colloids deposited in the secondary minimum. The shallowness of our calculated secondary minima, on the order of 10^{-3} k_BT, does not support the assertion that the depth of the secondary minima affects PRD1 attachment behavior.

We suggest that the secondary minimum need not have a large capacity for deposited colloids nor does it need to be deep for this interfacial

region to affect colloid transport. Colloids that primarily diffuse toward grain surfaces (as is the case for viruses) will move through a diffusion boundary layer, a region around the collector grain in which diffusive transport dominates over advective transport. Colloids in the boundary layer may approach the surface; however, under strongly repulsive conditions such as those encountered above the attachment edge, these colloids will not attach in the primary minimum. Instead, the viruses accumulate in the boundary layer in front of the energy barrier. In time, diffusion and advection will carry them out of the boundary layer and back to the advective flow. Regardless of the depth of the secondary minimum, the transport of these colloids has been retarded by reversible attachment. In our experiments, we surmise that the 5-10% of PRD1 that attached to quartz and Fe-quartz at pH values above the attachment edge were situated in the diffusion boundary layer created by draining the static column suspension.

4.3. Electrostatic control on virus attachment

The agreement between these experimental results and DLVO profiles suggest that viruses can overcome double layer repulsion to attach irreversibly in the primary minimum. For PRDI, such behavior has been attributed to hydrophobic forces driving attachment [23]. Additional forces based on hydrophobic exclusion of the viruses from the bulk suspension are not necessary to describe our results. In our PRD1-quartz experiments, irreversible attachment occurs at pH 5 even though both the virus and quartz surfaces are negatively charged. Likewise, irreversible deposition occurs in the Fe-quartz system where barriers exist at pH 6 and pH 6.6. It appears that the relatively low zeta potential of the PRDI is insufficient to prevent irreversible attachment at pH values below the attachment edge. It should be noted that the amendment of a silica surface by the addition of hydrocarbon chains [23] will decrease the negative surface charge of the silica surface in addition to providing a potential hydrophobic "harbor" for virus attachment. Increased virus attachment may be more reasonably attributed to the decrease in double layer repulsion rather than hydrophobic expulsion of the viruses from solution.

4.4. Repulsive barriers and attachment equilibrium

Significant repulsive energy barriers exist at some pH values below the attachment edges (e.g. pH 5 in the PRD1-quartz system). Because the rate of colloid attachment to surfaces is predicted to be exponentially dependent on the size of the repulsive energy barrier E25], the presence of a primary maximum in the DLVO profile is expected to dramatically slow the rate of virus attachment. Despite the presence of repulsive energy barriers of up to 20 k_BT, virus attachment appears to have reached equilibrium within the 5 h duration of the experiment. In fact, kinetic experiments revealed that attachment at pH values below the attachment edge was fast, on the order of less than 1 h [33]. Many studies have shown that experimental colloid deposition rates are much faster than deposition rates predicted based on the size of the energy barrier [55-58], so this discrepancy between the relatively short times necessary to achieve equilibrium and the presence of significant repulsive energy barriers is not surprising.

The DLVO profiles calculated with the Born potentials for both the PRD1-quartz and PRD1-Fe-quartz systems show transitions from attractive primary minima to repulsive primary minima at pH values very close to the pH values at which reversibility began to occur. As observed for attachment, it appears that the potential energy of the primary minimum relative to the potential energy of the bulk suspension dictates the equilibrium distribution of the viruses. Viruses attached at low pH are attached in primary minima located at attractive potential energies. These viruses remain attached until the increase in pH elevates the primary minimum to repulsive potential energies. When the primary minimum is elevated to a repulsive potential energy, the viruses attached in the primary minimum detach to re-establish the appropriate equilibrium distribution between the surface and the bulk solution.

The DLVO profiles cut off at the minimum separation distance of 1 nm cannot be used to explain the data. Based on the relative potential

energies of the primary minimum and the bulk solution, reversible attachment would be expected at a pH value between 3 and 5 for PRD1-quartz and between 5.9 and 6.6 for PRD1-Fe-quartz. These predictions clearly do not match the experimental results.

Using the DLVO profiles calculated with the Born potentials, the expected kinetics of virus transport over the energy barrier again appear to be violated. Just as viruses approaching the surface appear to overcome the repulsive energy barrier (- (ϕ_{max} - ϕ_{min2}) much faster than expected, viruses vacating the primary minimum appear to overcome the repulsive barrier to detachment (- (ϕ_{max} - ϕ_{min1}) quickly. If actual colloid deposition rates are always more rapid than predicted deposition rates, as noted above, it is conceivable that actual colloid transport in the opposite direction, detachment, could also occur more rapidly than expected.

4.5. Relating PRD1 attachment behavior to mineral surface chemistry

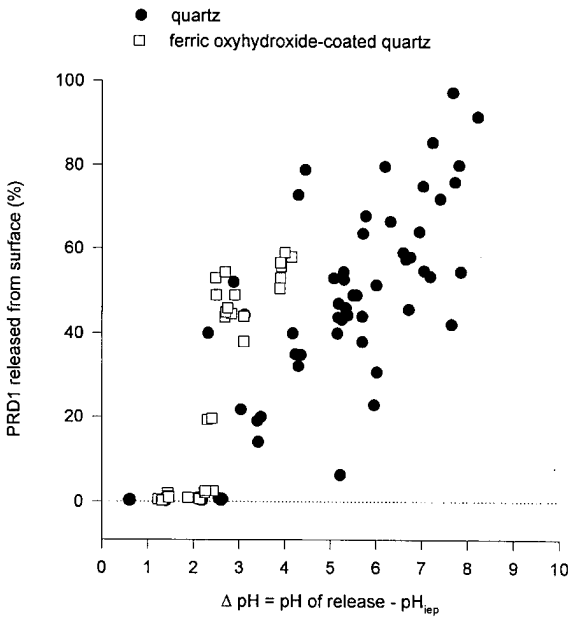

Fig. 9. Detachment of PRD1 from both mineral surfaces as a function of ΔpH, the difference between the measured detachment pH and the pH_{IEP} of the mineral surface.

The detachment of PRD1 from the quartz grains begins to occur at a pH value of about 4.9–5.5, or 2.4–3.0 pH units above the expected pH_{IEP} of the quartz grains. The detachment of PRD1 from the Fe–quartz grains began to occur at pH 7.5 ($\pm$ 0.1), about 2.4 pH units above the measured pH_{IEP} of the ferric oxyhydroxide-coated quartz grains. We surmise that the difference between the pH at which detachment begins and the pH_{IEP} of the mineral ($pH_{detach} - pH_{IEP} = \Delta pH$), is slightly greater for the PRD1–quartz system because PRD1 is slightly more negatively charged at pH 7.6 than it is at pH 5.5. At pH 7.5, the repulsion between the virus and Fe–quartz surface is about the same as that between the virus and quartz surfaces at pH 5.5. The highlighted curves at pH 5.5 for quartz and pH 7.5 for the Fe–quartz (Fig. 6) represent the DLVO profiles where PRD1 detachment was observed to initiate; note that these two DLVO profiles are quite similar. The PRD1 detachment results can be normalized to ΔpH to show that detachment from the two mineral surfaces occurs at approximately the same ΔpH value, about 2.5 (Fig. 9). The apparent difference in the slopes of these data may be attributed to the difference in the magnitude of the PRD1 surface charge at the different pH values.

Efforts to model virus transport in groundwater will be aided by the observation that the pH at which reversibility of virus-mineral attachment will occur can be normalized to the pH_{IEP} of the aquifer media. For **PRD1,** attachment became reversible at ΔpH = 2.4-3.0 pH units above the mineral pH_{IEP} values. Further investigation is required for viruses with different pH_{IEP} values. The pH_{IEP} of PRD I is on the low end of virus pH_{IEP} values; for example, Murray and Parks [13] reported poliovirus pH_{IEP} values of about 6.6 for infectious poliovirus and ≤ 5.7 for non-infectious poliovirus. If the pH_{IEP} Of the virus increases, the virus surface charge will be less negative at any given pH; therefore, the mineral surface charge will have to be more negative to promote reversible attachment. For this to occur, a higher value of ΔpH will be necessary. If the surface properties of both the virus and mineral surfaces are known, it should be possible to construct regions of virus attachment behavior (e.g. irreversible attachment, reversible attachment, no

attachment) based on the pH_{IEP} values of the viruses and minerals. Currently, the surface properties of many enteric viruses, like hepatitis A, Norwalk, and human immunodeficiency viruses, are not known.

4.6. Alternative DLVO calculations

Our virus attachment data agree well with the calculated DLVO profiles if we interpret the equilibrium distributions of the viruses by the position of the primary minimum relative to 0 "' = 0; however, there are many uncertainties involved in the DLVO calculations. The size of the secondary minimum is especially sensitive to ionic strength and the magnitude of the double layer potential energy. The HHF expression [41] that we used to calculate the double layer potential energy is an approximate solution of the Poisson-Boltzman equation. Adaptations of the HHF expression to sphere-sphere and sphere-plate geometries are also approximations. More accurate expressions of the double layer potential energy have been derived (see, for example, Refs. [59-60]) and some of these expressions provide more accurate fits to measured surface forces [61]. According to comparisons with measured surface forces, the HHF double layer expression over predicts the repulsive force between surfaces. At the relatively small zeta potentials encountered on the mineral and virus surfaces in this work, the error between the HHF double layer potential and the actual potential is not expected to be large; however, correction of this error would decrease the size of the repulsive energy barrier that must be overcome to achieve equilibrium and increase the depth of the secondary minima.

Some of the critical parameters inserted into the potential energy calculations may be inaccurate. First, the use of zeta potentials as surface potentials in the double layer potential energy calculation may underestimate actual surface potentials and the double layer potential energy. Combining the use of zeta potentials with the use of a minimum separation distance should minimize this error; however, our attachment data do not agree with the DLVO profiles cut off at the minimum separation distance of I nm. We must also consider the possibility of inaccuracy of the measured zeta potentials. Our measurement of the zeta potential of the fine particles isolated from the quartz and Fe-quartz grains may have introduced some bias into the double layer potential energy calculations if these particles were not representative of the grain surfaces. The PRD1 zeta potentials were obtained by Bales et al. [23] in the presence of the potential-determining ions calcium and phosphate, while our experiments were conducted in the presence of electrolytes not expected to affect the virus surface potentials, sodium nitrate and the biological buffers.

Second, the Hamaker constants chosen for the calculation of the van der Waals potential energy for these systems were taken from Murray and Parks' [13] estimates for poliovirus-mineral systems. If the Hamaker constants are too high, the DLVO profiles are too attractive; if the Hamaker constants are too low, the DLVO profiles are too repulsive.

Third, the Born collision parameters chosen for the calculation of the Born potential was taken as the same value used by Ruckenstein and Prieve [25] and Barouch et al. [45]. According to Feke et al. [44], the value of a= 5A was obtained as a fitting parameter for interatomic potentials. Ryan and Gschwend [22] adjusted the collision parameter to 20 A to fit colloid release data for a hematite colloid-quartz grain system. If the collision parameter is too low, then the depth of the primary minimum has been overestimated.

Fourth, the implementation of DLVO theory assumes that the surfaces are homogeneously charged, an assumption that is unlikely to be true. Recently, the charge heterogeneity of porous media surfaces has been cited as an explanation for measured colloid deposition rates far in excess of those predicted using DLVO energy barriers [62]. The microscopic variability in grain mineralogy leading to charge heterogeneity probably poses an even greater problem in the interpretation of the detachment results using DLVO energy barriers. The microscopic variability will also give rise to heterogeneity in the Hamaker constant, which would lead to significant variations in the Born repulsion at the short separation distances that control the depth of the primary minimum.

4.7. Implications of reversibility on virus transport predictions

Virus transport through aquifers has been modeled using irreversible attachment terms, reversible "adsorption" terms, and combinations of the two terms [23,24,63-66]. The time scales for irreversible and reversible attachment are only important relative to the time scales for groundwater flow. The irreversible attachment terms are borrowed from colloid filtration theory, in which colloid deposition onto collector grains is assumed to be fast and irreversible [17]. Irreversible attachment will reduce the number of mobile viruses and may completely remove the mobile viruses if enough attachment sites are available along the flow path from the virus source to an affected wellhead. Irreversible attachment will not decrease the velocity of the viruses that avoid attachment. Because irreversible attachment does not retard the transport of viruses that avoid attachment, additional time for virus removal by inactivation is not provided. For virus transport, the arrival of only 2 viruses per 107 1 of water is a cause for regulatory concern [67]; therefore, irreversible attachment of viruses may not provide optimal protection for wellheads if virus inactivation is the primary virus removal mechanism.

Reversible "adsorption" of viruses to mineral surfaces implies that virus transport is retarded but not attenuated. If virus attachment to aquifer grains is completely reversible, eventually all viruses will reach the affected wellhead; however, their average transport time from the virus source to the wellhead will be greater than that of the groundwater. This retardation affords additional time for virus removal by inactivation.

In many cases, virus and bacteria breakthrough data have been best fit by a combination of both irreversible and reversible attachment terms [23,28]. For virus transport through a homogeneous porous medium, the application of the two attachment terms allows the virus breakthrough data to be accurately fit; however, virus attachment to the homogeneous porous media does not justify the application of two attachment processes. Our results suggest that virus attachment to a homogeneous mineral surface will be either irreversible or reversible depending on the pH of attachment, but not both. For virus transport through a heterogeneous porous medium, such as that encountered in the bacteria transport field test conducted by Harvey and Garabedian [28], the application of two attachment terms may be justified by the existence of different minerals to which bacteria attachment may be irreversible or reversible; e.g. quartz and ferric oxyhydroxide at a pH value between the pH_{IEP} values of the two minerals.

5. Conclusions

PRD1 attachment to quartz and ferric oxyhydroxide-coated quartz is characterized by attachment "edges" that occur at a pH value about 2.5-3.5 units above the pH_{IEP} of the mineral surfaces. Below this pH, PRD1 attachment is nearly complete and irreversible. Above this pH, PRD1 attachment is minimal and reversible. PRD1 attached at pH values below the attachment edge can be detached by increasing the pH of the detachment solution to a pH above the attachment edge.

The attachment "edge" occurred at a pH that produces DLVO primary minima located at potential energies near zero. At pH values below the attachment edge, the primary minima are negative, or produce attractive potential energies. At pH values above the attachment edge, the primary minima are positive, or repulsive. The equilibrium distribution of PRD1 between the primary minimum and the bulk suspension appears to be dictated by the potential energy of the primary minimum. Equilibrium distributions were achieved in less than 5 h despite the presence of significant repulsive energy barriers to both attachment and detachment.

The PRD1 attachment behavior and its correlation to DLVO potential energy profiles suggest that viruses attached below the attachment edge are attached irreversibly in the primary minimum. Viruses attached in the primary minimum may be detached by a small increase in pH, as evidenced by sharp demarcation in the irreversible to reversible virus attachment with increasing pH. The viruses reversibly attached above the attachment

edge would be attached in secondary minima; however, our DLVO calculations produced secondary minima too shallow to explain virus attachment. Instead, we hypothesize that these viruses temporarily reside in the diffusion boundary layer around porous media grains created by sampling the static columns.

Acknowledgements

The authors thank the National Water Research Institute and the U.S. Environmental Protection Agency for their support of this project under grant HRA 699-514-92. Philip Berger of the U.S. EPA provided valuable assistance in understanding regulatory aspects of virus transport. We are also grateful to Karla Kirkegaard, Connie Nugent, and Mali Illangasekare of the Department of Molecular, Cellular, and Developmental Biology, University of Colorado, Boulder, for their technical assistance and use of ultracentrifuges. Several project chiefs at the United States Geological Survey's Boulder laboratory provided access to equipment, including George Aiken, Diane McKnight, Howard Taylor, Dick Smith, and Dennis Eberl. Two anonymous reviewers provided helpful comments. Finally, we extend special thanks to Dave Metge of the USGS and Annie Pieper of the University of Colorado for their contributions in the laboratory.

References

[1] USEPA, Guidelines for Delineation of Wellhead Protection Areas, United States Environmental Protection Agency, Office of Ground-Water Protection, Washington, DC, 1987.
[2] P. Berger, in U. Zoller (Ed.), Ground Water Contamination and Control, Marcel Dekker, New York, 1994, p. 645.
[3] B.H. Keswick and C.P. Gerba, Environ. Sci. Technol., 14 (1980) 1290.
[4] C.P. Gerba and J.C. Lance, Appl. Environ. Microbiol., 36 (1978) 247.
[5] G.F. Craun, in G.F. Craun (Ed.), Water Diseases in the United States, CRC Press, Boca Raton, 1986, p. 73.
[6] W.D. Burge and N.K. Enkiri, J. Environ. Qual., 7 (1978) 73.
[7] E.F. Landry, J.M. Vaughn, M.Z. Thomas and C.A. Beckwith, Appl. Environ. Microbiol., 38 (1979) 680.
[8] R.S. Moore, D.H. Taylor, M.M.M. Reddy and L.S. Sturman, Appl. Environ. Microiol., 44 (1982) 852.
[9] K.S. Zerda, C.P. Gerba, K.C. Hou and S.M. Goyal, Appl. Environ. Microbiol., 49 (1985) 91.
[10] M.D. Sobsey, P.A. Shields, F.H. Hauchman, R.L. Hazard and L.W. Caton, III, Water Sci. Technol., 18 (1986) 97.
[11] C.P. Gerba, in A.I. Laskin (Ed.), Advances in Applied Microbiology, Vol. 30, Academic Press, New York, 1984, p. 133.
[12] S.G. Goyal and C.P. Gerba, Appl. Environ. Microbiol., 38 (1979) 241.
[13] J.P. Murray and G.A. Parks, in M.C. Kavanaugh and J.O. Leckie (Eds.), Particulates in Water: Characterization, Fate, Effects and Removal, Adv. Chem. Ser. 189, American Chemical Society, Washington, DC, 1978.
[14] E.F. Landry, J.M. Vaughn and W.F. Penello, Appl. Environ. Microbiol., 40 (1980) 1032.
[15] R.S. Moore, D.H. Taylor, L.S. Sturman, M.M. Reddy, and G.W. Fuhs, Appl. Environ. Microbiol., 42 (1981) 963.
[16] C.P. Gerba, S.M. Goyal, I. Cech and G.F. Bogdan, Environ. Sci. Technol., 15 (1981) 940.
[17] K.M. Yao, M.T. Habibian and C.R. O'Melia, Environ. Sci. Technol., 5 (1971) 1105.
[18] R. Rajagopalan and C. Tien, AIChE J., 22 (1976) 523.
[19] B.V. Derjaguin and L.D. Landau, Acta Physicochim. URSS, 14 (1941) 633.
[20] E.J.W. Verwey and J.Th. G. Overbeek, Theory of the Stability of Lyophobic Colloids, Elsevier, Amsterdam, 1948.
[21] N. Kallay, E. Barouch and E. Matijević, Adv. Colloid Interface Sci., 27 (1987) 1.
[22] J.N. Ryan and P.M. Gschwend, J. Colloid Interface Sci., 164 (1994) 21.
[23] R.C. Bales, S.R. Hinkle, T.W. Kroeger, K. Stocking and C.P. Gerba, Environ. Sci. Technol., 25 (1991) 2088.
[24] R.C. Bales, S. Li, K.M. Maguire, M.T. Yahya and C.P. Gerba, Water Resour. Res., 29 (1993) 957.
[25] E. Ruckenstein and D.C. Prieve, AIChE J., 22 (1976) 276.
[26] A. Marmur, J. Colloid Interface Sci., 72 (1979) 41.
[27] P. Ludwig and G. Peschel, Prog. Colloid Polym. Sci., 77 (1988) 146.
[28] R.W. Harvey and S.P. Garabedian, Environ. Sci. Technol., 25 (1991) 178.
[29] IAWPRC Study Group on Health Related Water Microbiology, Water Res., 25 (1991) 529.
[30] R.H. Olsen, J. Siak and R.H. Gray, Virology, 14 (1974) 689.
[31] L. Mindich, D. Bamford, T. McGraw and G. MacKenzie, Virology, 44 (1982) 1021.
[32] M.H. Adams, Bacteriophages, Interscience, New York, 1959.
[33] J.P. Loveland, M.Sc. Thesis, University of Colorado, Boulder, CO, 1995.
[34] J. Charney, R. Machlowitz, A.A. Tytell, J.F. Sagin and D.S. Spicer, Virology, 15 (1961) 269.

[35] W.K. Joklik and J.E. Darnell, Jr., Virology, 13 (1961) 439.
[36] J.K.H. Bamford and D.H. Bamford, Virology, 181 (1991) 348.
[37] M.A. Scholl and R.W. Harvey, Environ. Sci. Technol., 26 (1992) 1410.
[38] M. Edwards and M.M. Benjamin, J. Water Pollut. Control Fed., 61 (1989) 1532.
[39] A.P. Pieper, M.Sc. Thesis, University of Colorado, Boulder, CO, 1995.
[40] M. Elimelech and C.R. O'Melia, Langmuir, 6 (1990) 1153.
[41] R. Hogg, T.W. Healy and D.W. Fuerstenau, Faraday Soc. Trans., 62 (1966) 1638.
[42] J. Gregory, J. Colloid Interface Sci., 83 (1981) 138.
[43] D. Bargeman and F. van Voorst Vader, J. Electroanal. Chem., 37 (1972) 45.
[44] D.L. Feke, N.D. Prabhu, J.A. Mann, Jr. and J.A. Mann, III, J. Phys. Chem., 88 (1984) 5735.
[45] E. Barouch, E. Matijević and T.H. Wright, Chem. Eng. Commun., 55 (1987) 29.
[46] J.N. Israelachvili and G.E. Adams, J. Chem. Soc. Faraday Trans. 1, 74 (1978) 975.
[47] R.J. Hunter, Zeta Potential in Colloid Science, Principles and Applications, Academic Press, New York, 1981.
[48] G. Frens and J.Th.G. Overbeek, J. Colloid Interface Sci., 38 (1972) 376.
[49] J.E. Kolakowski and E. Matijević, J. Chem. Soc. Faraday Trans. 1, 75 (1979) 65.
[50] R.J. Kuo and E. Matijević, J. Chem. Soc. Faraday Trans. 1, 75 (1979) 2014.
[51] N. Kallay, B. Biškup, M. Tomić and E. Matijević, J. Colloid Interface Sci., 114 (1986) 357.
[52] G.A. Parks, Chem. Rev., 67 (1965) 177.
[53] S.B. Grant, Environ. Sci. Technol., 28 (1994) 928.
[54] M.T. Yahya, L. Galsaomies, C.P. Gerba and R.C. Bales, Water Sci. Technol., 27 (1993) 409.
[55] M. Hull and J.A. Kitchener, Trans. Faraday Soc., 65 (1969) 3093
[56] B.D. Bowen and N. Epstein, J. Colloid Interface Sci., 72 (1979) 81.
[57] J. Gregory and A. Wishart, Colloids Surfaces, 1 (1980) 313.
[58] M. Elimelech, Water Res., 26 (1992) 1.
[59] H. Oshima, D.Y.C. Chan, T.W. Healy and L.R. White, J. Colloid Interface Sci., 92 (1983) 232.
[60] J.Th.G. Overbeek, Colloids Surfaces, 51 (1990) 61.
[61] H. Kihira and E. Matijević, Adv. Colloid Interface Sci., 42 (1992) 1.
[62] L. Song and M. Elimelech, J. Colloid Interface Sci., 167 (1994) 301.
[63] M.Y. Corapcioglu and A. Haridas, J. Hydrol., 72 (1984) 149.
[64] M.V. Yates, S.R. Yates, J. Wagner and C.P. Gerba, J. Contaminant Hydrol., 1 (1987) 329.
[65] N.S. Park, T.N. Blandford and P.S. Huyakorn, VIRALT, Version 2.1, International Ground Water Modeling Center, Colorado School of Mines, Golden, CO, 1992.
[66] N.S. Park, T.N. Blandford and P.S. Huyakorn, CANVAS, A Composite Analytical–Numerical Model for Viral and Solute Transport Simulation, HydroGeoLogic, Inc., Herndon, VA, 1993.
[67] S. Regli, J.B. Rose, C.N. Haas and C.P. Gerba, J. Am. Water Works Assoc., 83 (1991) 76.